NRC Research Press

ARTICLE

Ice wedge degradation and CO_2 and CH_4 emissions in the Tuktoyaktuk Coastlands, Northwest Territories

Abra F. Martin, Trevor C. Lantz, and Elyn R. Humphreys

Abstract: Increases in ground temperature make soil organic carbon in permafrost environments highly vulnerable to release to the atmosphere. High-centred polygonal terrain is a form of patterned ground that may act as a large source of carbon to the atmosphere because thawing ice wedges can result in increased ground temperatures, soil moisture, and thaw depth. To evaluate the effect of ice wedge degradation on carbon flux, carbon emissions were characterized at two polygonal peatlands in the Tuktoyaktuk Coastlands in northern Canada. Opaque chambers were used to measure CO_2 and CH_4 emissions from nine nondegraded polygon centres and nine moderately degraded troughs four times during the growing season. To measure emissions from 10 ponds resulting from severe ice wedge degradation, wind diffusion models were used to characterize fluxes using CO_2 and CH_4 concentration measurements made in each pond. Our field data show that degraded troughs had increased ground temperature, deeper active layers, and increased CO_2 and CH_4 emissions. Our study shows that rates of CO_2 and CH_4 emissions from high-centreed polygonal terrain are likely to increase with more widespread melt pond formation in this terrain type.

Key words: carbon dioxide, methane, permafrost, thermokarst.

Résumé : Les augmentations de la température au sol rendent le carbone organique du sol dans les milieux de pergélisol fortement vulnérables à être rejeté dans l'atmosphère. Le terrain de polygones convexes est une forme de sol géométrique qui peut comprendre des zones qui agissent comme de grandes sources de carbone à l'atmosphère parce que le dégel des coins de glace peut produire des augmentations de température au sol, d'humidité du sol et de profondeur de dégel. Dans le but d'évaluer l'effet de dégradation des coins de glace sur le flux de carbone, les émissions de carbone ont été caractérisées à deux tourbières polygonales dans la zone côtière du Tuktoyaktuk au nord du Canada. Des chambres opaques ont été utilisées pour mesurer les émissions de CO_2 et de CH_4 de neuf centres de polygones non dégradés et de neuf dépressions modérément dégradées, et ce, quatre fois pendant la saison de croissance. Dans le but de mesurer les émissions de 10 étangs en raison de la grave dégradation de coins de glace, les modèles de diffusion de vent ont été utilisés afin de caractériser les flux utilisant des mesures de CO_2 et de CH_4 prises dans chaque étang. Nos données de terrain montrent que les dépressions dégradées avaient donné lieu à l'augmentation de la température du sol, des couches actives plus profondes et à des émissions de CO_2 et de CH_4 accrues. Notre étude indique que les taux d'émissions de CO_2 et de CH_4 provenant de terrain de polygones convexes

Received 2 May 2016. Accepted 26 September 2017.

A.F. Martin and T.C. Lantz. School of Environmental Studies, University of Victoria, Victoria, BC V8P 5C2, Canada.
E.R. Humphreys. Geography and Environmental Studies, Carleton University, Ottawa, ON K1S 5B6, Canada.
Corresponding author: Trevor C. Lantz (e-mail: tlantz@uvic.ca).

vont probablement augmenter avec la formation plus répandue d'étangs de fonte dans ce type de terrain. [Traduit par la Rédaction]

Mots-clés : dioxyde de carbone, méthane, pergélisol, thermokarst.

Introduction

Permafrost soils hold large quantities (1140–1476 Pg) of soil organic carbon (Hugelius et al. 2014). Ongoing changes in temperature and precipitation are likely to alter carbon cycling in Arctic and subarctic ecosystems (Oechel et al. 1993; Schuur et al. 2008; Grosse et al. 2011) and thawing permafrost in the circumpolar region could release between 37 and 174 Pg of carbon to the atmosphere by 2100 (Schuur et al. 2015). It is estimated that the permafrost carbon feedback could result in an additional 0.42 °C of warming by 2300 (Schuur et al. 2015).

High-centred polygonal terrain is one of the most common forms of patterned ground in the Low Arctic. This terrain type is characterized by thick organic deposits and large ice wedges (Zoltai and Tarnocai 1975; Vardy et al. 1997). Elevated polygon centres are surrounded by low-lying troughs underlain by ice wedges, which form a characteristic polygonal network when viewed from above (Figs. 1A and 1B). Common in low-lying lacustrine basins across the Arctic, high-centred polygon terrain is likely to be particularly sensitive to climate warming because the ground ice content is high (Kokelj et al. 2014). When ice wedges degrade, the ground subsides, polygon troughs become wetter, and active layer thickness and mean annual ground temperature increase (Jorgenson et al. 2015). Moderate trough degradation is characterized by some subsidence, increased moisture, and the presence of sedges (Fig. 1D). Terrain subsidence associated with severe ice wedge degradation results in the formation of melt ponds that do not support rooted plants (Figs. 1E and 1H). The volume and depth of water in these ponds may extend the duration of freeze-back, and in some locations the underlying soil may not freezeback over winter (Kokelj et al. 2014). Several recent studies show that ice wedge degradation in high-centred polygonal terrain is increasing the number and size of melt ponds at sites across the Arctic (Raynolds et al. 2014; Jorgenson et al. 2015; Liljedahl et al. 2016; Steedman et al. 2017).

Increased ice wedge degradation has the potential to affect 10%–30% of Arctic lowlands (Jorgenson et al. 2006) and the changes in soil moisture that accompany degradation are likely to have a significant impact on carbon cycling (Schuur et al. 2008; Lee et al. 2010; Kokelj and Jorgenson 2013). As ice wedges degrade, adjacent soils become saturated and aerobic decomposition processes may become limited as diffusion of oxygen belowground is restricted (Funk et al. 1994; Davidson and Janssens 2006; Schlesinger and Bernhardt 2013). Anaerobic conditions are likely to promote CH_4 production (Schlesinger and Bernhardt 2013). Other studies have shown that small water bodies can have substantial emission rates for both CO_2 and CH_4 (Bouchard et al. 2015). With the formation of melt ponds in severely degraded ice wedges, microbial activity in the water column and the soils underlying the ponds may promote emissions of both CO_2 and CH_4 via diffusion or ebullition to the surface (Laurion et al. 2010). Increased temperature, moisture, thaw depths, and substrate availability resulting from ice wedge degradation is also likely to result in increased anaerobic production of both CO_2 and CH_4. In this research, we tested the hypothesis that ice wedge degradation results in larger summer emissions of both CO_2 and CH_4 by emissions from severely degraded troughs (melt ponds), moderately degraded troughs (wet troughs), and nondegraded areas (polygon centres).

Fig. 1. Photographs showing study sites and degradation classes. (A) Subarctic field site near Inuvik; boardwalks are to the left of where chamber measurements occurred. (B) Arctic field site near Tuktoyaktuk; the two orange lines are snow fences for another research project. (C) Polygon centre with no ice wedge and no degradation. (D) Shallow trough produced as a result of moderate ice wedge degradation. (E) Pond resulting from severe ice wedge degradation. (F) Gas sampling collar in a polygon centre. (G) Gas sampling collar in a shallow trough. (H) Close-up view of a melt pond.

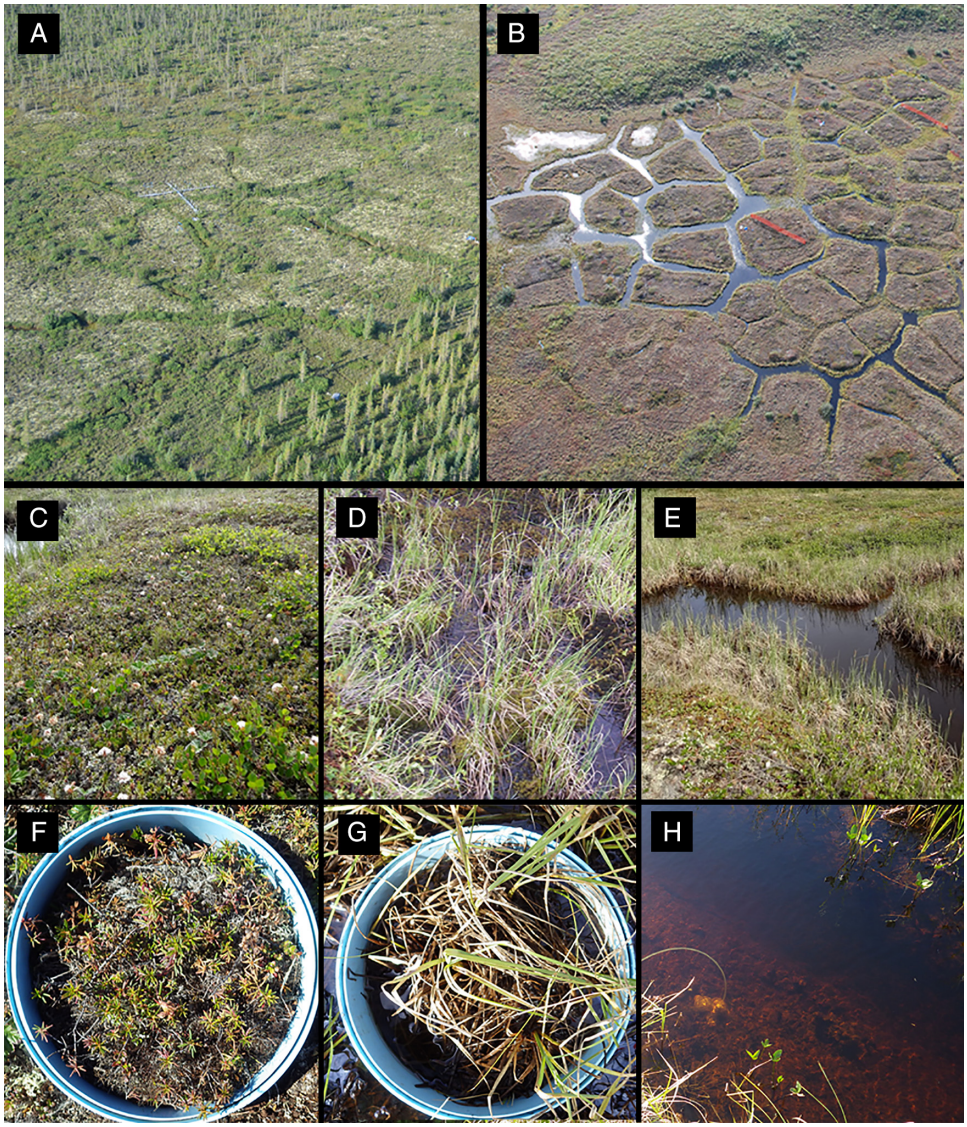

Methods

Study area

This study was carried out in the Tuktoyaktuk Coastlands in the western Canadian Arctic (Fig. 2). This area is characterized by gentle topography and thousands of small lakes (Rampton 1988). Between 30 and 25 ka B.P., the Tuktoyaktuk Coastlands were covered by the Laurentide ice sheet (Duk-Rodkin and Lemmen 2000). As this ice sheet

Fig. 2. Map of the study area showing study sites, nearby communities, and ecoregion boundaries.

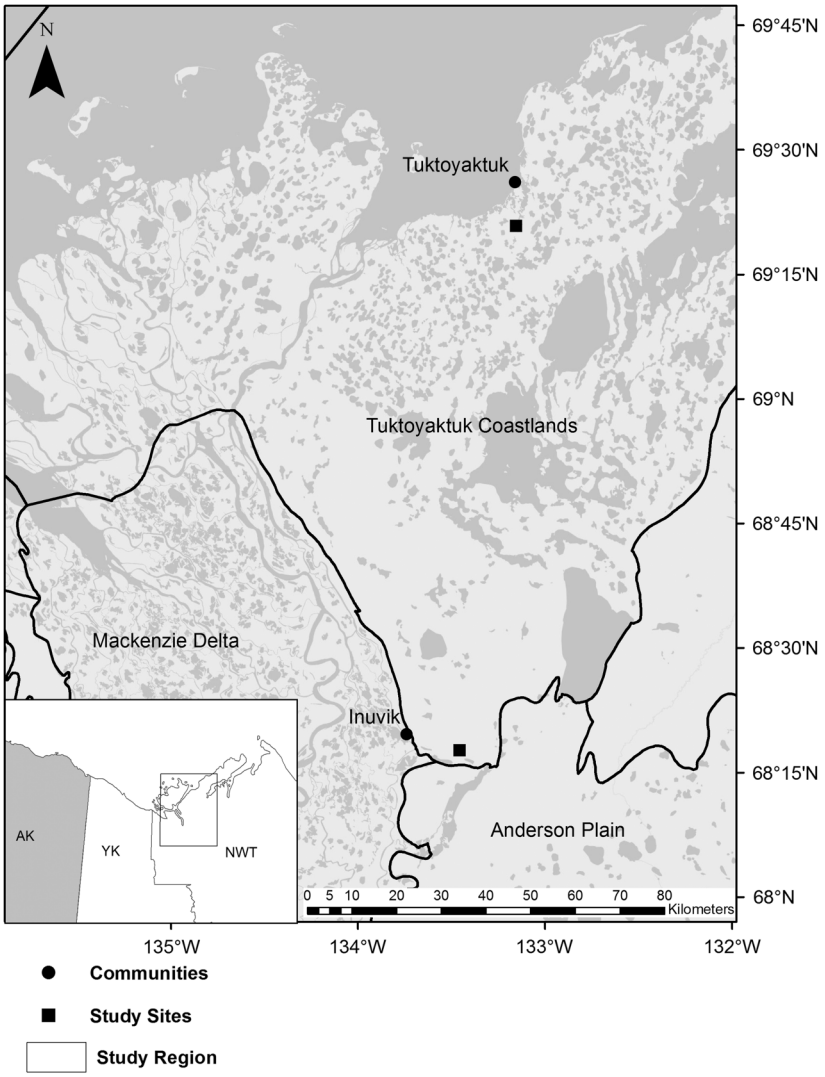

receded, numerous lakes formed, many of which subsequently drained during the Holocene (Murton 1996). Today, approximately 10% of the Tuktoyaktuk Coastlands are occupied by small basins that host high-centred polygon terrain underlain by thick peat deposits (Zoltai and Tarnocai 1975; Vardy et al. 1997; Lantz et al. 2017; Steedman et al. 2017).

The contemporary climate of this region is characterized by mean annual air temperatures of −9.0 °C at Inuvik and −10.2 °C at Tuktoyaktuk, and temperatures typically below freezing from October to April (Environment Canada 2015). In the summer, there is a strong latitudinal temperature gradient across the Tuktoyaktuk Coastlands with average growing season air temperatures (1970–2005) being 3.3 °C warmer in Inuvik than in Tuktoyaktuk (Lantz et al. 2010*a*). There is also a precipitation gradient with Tuktoyaktuk receiving a mean total annual precipitation (1970–2006) of 166.1 mm and Inuvik receiving 254.8 mm

(Environment Canada 2015). Between 1926 and 2006, mean annual air temperatures at Inuvik increased by 1.9 °C (Lantz and Kokelj 2008). This increase in air temperature has been mirrored by an increase in ground temperature of 1.5–2.5 °C since 1970 (Burn and Kokelj 2009; Kokelj et al. 2017).

The regional climate gradient is accompanied by two transitions in the dominant vegetation. In the southern part of the study area, open spruce woodlands transition into tundra dominated by upright shrubs (*Salix* spp., *Alnus viridis* Chaix., and *Betula glandulosa* Michx.). Towards the northern end of our study area, upright shrub tundra is replaced by dwarf shrub tundra dominated by ericaceous shrubs and sedges (*Rhododendron subarcticum* Harmaja (G.D. Wallace), *Vaccinium vitis-idaea* L., *Carex* spp., and *Eriophorum* spp.) (Lantz et al. 2010*b*).

Study sites

The effect of ice wedge degradation on soil respiration was measured at a subarctic site near the community of Inuvik, Northwest Territories (68°18′55.67″N, 133°25′53.51″W), and an Arctic site near Tuktoyaktuk, Northwest Territories (69°21′58.08″N, 133°2′6.29″W). Each site was located in an area with high-centred polygons dominated by dwarf shrubs (*B. glandulosa*, *R. subarcticum*, *V. vitis-idaea*, *Vaccinium uliginosum* L., *Empetrum nigrum* L.), sedges (*Eriophorum* spp., *Carex aquatilis* Wahlenb.), and lichen. Both sites had areas differentially affected by degradation. We classified these areas as (1) nondegraded areas without ice wedges (polygon centres), (2) moderately degraded ice wedges (wet troughs), and (3) highly degraded ice wedges (melt ponds) (Fig. 1). Polygon centres were characterized by terricolous lichen, *Rubus chamaemorus* L., *R. subarcticum*, and *V. vitis-idaea*. Wet troughs had standing water up to 10 cm deep and were typically dominated by *C. aquatilis*. Melt ponds were deeper and characterized by standing water roughly 10–90 cm deep and 12–305 cm wide (on average 172 cm wide) with an absence of rooted vegetation in the pond centres. All melt ponds at our subarctic site had floating moss mats, whereas moss was absent in all of our Arctic melt ponds (Figs. 1E and 1H).

Hourly temperature and measurements

In 2012, two polygon centres, three wet troughs, and two melt ponds at each field site were instrumented with temperature sensors. Temperature measurements (5, 50, and 100 cm) were made every 2 h using temperature sensors (Onset Computing, HOBO™, TMC20-HD, accuracy ±0.25 °C) attached to data loggers (Onset Computing, HOBO™, U12-008 and H21-002).

Gas sampling

At each of the two study sites, we measured CH_4 and CO_2 fluxes at nine replicate polygon centres, nine replicate wet troughs, and 10 replicate melt ponds. For the polygon centres and wet troughs, we used manual, static, non-steady-state chambers (see Bubier et al. 1995). These collars consisted of PVC pipes 24.3 cm in diameter and 30 cm tall that were installed to a depth of 25 cm (Figs. 1F and 1G). The top of the collars were grooved and filled with water during sampling to create an air-tight seal with the sampling chamber. Chambers were 34 cm tall and constructed of polycarbonate, made opaque using black duct tape to limit photosynthesis, and fitted with a vent consisting of a 10 cm coiled 3.18 mm diameter copper pipe to maintain constant pressure during sampling. During the growing season, CO_2 and CH_4 fluxes were measured between the hours of 11:00 and 16:00 at the subarctic site on 27 June, 17 July, 31 July, and 21 August and at the Arctic site on 3 July, 12 July, 29 July, and 15 August 2013. Average air temperature on those four dates was 14.1 ± 5.3 °C at the subarctic site and 12.1 ± 5.2 °C at the Arctic site.

Sampling involved sealing the chamber into the water-filled collar groove and drawing a 24 mL sample from the chamber through a line fitted with a septum attached to a three-way luer stopcock at 0, 10, 20, and 30 min. Before drawing the air from the chamber, air in the chamber volume was mixed by pumping the syringe attached to the gas sampling line five times. This method of mixing creates air movement within the chamber volume when the air is forcibly pushed back into the volume via a larger 60 cc syringe. Air samples were transferred into pre-evacuated vials with a small amount of magnesium perchlorate as a desiccant (Exetainer 739B Labco Ltd., Buckinghamshire, UK). Ambient air samples were also taken at 1 m above the ground surface to provide a reference point that could be used to verify that samples were not damaged in transport. Four measurements of temperature 5 cm below the surface (either soil or water surface) were taken around each collar in the polygon centres and wet troughs. Four measurements of soil moisture integrated between 0 and 6.8 cm from the surface (water or soil) were also taken during sampling at each of these collars. The moisture measurements were taken using a soil moisture probe (type WET-2, Delta-T, Cambridge, UK) calibrated using the organic soils at each site. Water table depth was determined for each collar in a wet trough by measuring the height from the top of the soil to the surface of any standing water. In late August 2013, measurements of active layer thickness were made at both the Arctic and subarctic sites by setting up a 10 m by 10 m grid, with 110 evenly spaced sampling points and using an active layer probe, which was pushed into the ground to the depth of refusal. In the case of melt ponds where standing water was present, thaw depth was measured relative to the base of the pond by lowering the probe to the base of the pond, recording this distance (A), and then pushing the probe until it met resistance and measured this distance (B). Thaw depth was calculated as $B - A$. Using this grid design, estimates of active layer depth were collected for polygon centres (each site $n = 27$), wet troughs (subarctic $n = 15$, Arctic $n = 19$), and melt ponds (subarctic $n = 3$, Arctic $n = 10$).

We used two approaches to estimate gas emissions from melt ponds. At each site, we installed ten 15.24 cm diameter funnels to collect gas bubbles produced at the bottom of the ice wedge ponds. Each funnel was equipped with a sampling line ending in a three-way luer-lock stopcock and was secured in pond sediments using a weight on the top of the funnel (Huttunen et al. 2001); however, these funnels did not collect sufficient gas for analysis (from one or two bubbles to 6 cm^3), suggesting that ebullition was a minor transport process for CO_2 and CH_4 emissions at these small melt ponds. We also estimated gas flux from ponds using the diffusion method (e.g., Laurion et al. 2010) by sampling surface water. At each pond, 30 mL of surface water was collected using a 60 mL syringe followed by 30 mL of ambient air. The contents of the water-filled syringe were shaken for 1 min to equilibrate the gas stored in the water with the air. Finally, 24 mL of this air was then transferred to a preevacuated vial for analysis. An ambient air sample was also taken to determine ambient CO_2 and CH_4 concentrations. Water temperature (5 cm below the surface) and water depth were measured at the time of sampling. Ambient air temperature, pressure, and wind speed at the time of sampling were obtained from an Environment Canada weather station 2.45 km from the subarctic site and 7.17 km from the Arctic site (Environment Canada 2015).

Gas samples were analysed for CO_2 and CH_4 on a gas chromatograph (CP 3800, Varian, California) with a methanizer and flame-ionization detector, which were operated at 350 and 300 °C, respectively. Helium was used as a carrier gas at 30 mL min^{-1}. Gas was separated using a Haysep N 80/100 precolumn (0.32 cm diameter × 50 cm length) and Poropak QS 80/100 mesh analystical columns (0.32 cm diameter × 200 cm length) in a column oven with a temperature of 50 °C. For each run, three replicates of five standards were used to maintain quality control and establish the linear relationship between

chromatogram area and gas concentration. Both the CO_2 and the CH_4 standards ranged from slightly below ambient concentration to 2.5%.

Gas flux estimates

The flux of CH_4 or CO_2 in the chambers was estimated from the change in gas concentration over the 30 min sampling interval:

$$\text{Flux} = \left(\frac{p_a V}{A}\right)\left(\frac{dx}{dt}\right)$$

where p_a is the density of dry air (mol m^{-3}, determined using ambient air temperature and pressure from the Environment Canada weather station), V is the volume of the chamber (0.0159 m^3 plus 0.002 m^3 for the volume within the collars to the surface of the soil or water), A is the area of the chamber (0.0464 m^2), and dx/dt is the rate of change of the mixing ratio of either CH_4 or CO_2 (μmol mol^{-1} s^{-1}).

To calculate CO_2 and CH_4 flux from the surface water samples, first the initial (P_i) and final (P_f) headspace partial pressures of CO_2 and CH_4 were calculated from the gas chromatograph readings (μmol mol^{-1}) and the atmospheric pressure at sampling (atm). Then, dissolved gas ($C_{[pw]}$) in the surface water samples (μmol L^{-1}) was determined using the following:

$$C_{[pw]} = P_f\left(\frac{V_h}{V_w RT}\right) - P_i\left(\frac{V_h}{V_w RT}\right) + K_H P_f$$

where K_H is the Henry's constant for CO_2 or CH_4 (mol L^{-1} atm^{-1}) calculated for freshwater using water temperature (T) following (Weiss 1974) and (Wanninkhof 1992), respectively, R is the ideal gas constant (L atm mol^{-1} K^{-1}), and V_h and V_w are the volumes of the headspace and water after equilibration (L) (Dinsmore 2008).

Flux across the water–air interface (μmol m^{-2} s^{-1}) was calculated using the thin boundary layer model using measurements of wind speed and gas concentrations in the air and water (Laurion et al. 2010):

$$\text{Flux} = k\left(C_{[pw]} - C_{[amb]}\right)$$

where $C_{[pw]}$ is the total pore water concentration in the surface water (μmol L^{-1}) and C_{amb} is the equilibrium ambient concentration of CO_2 or CH_4 in the atmosphere (μmol L^{-1}). The gas transfer velocity for each gas, k (cm h^{-1}), was empirically derived using the Schmidt number (Sc) and the normalized gas transfer velocity k_{600} following Cole and Caraco (1998):

$$k = k_{600}\left(\frac{Sc}{600}\right)^{-n}$$

$$k_{600} = 2.07 + 0.215 \times U_{10}^{1.7}$$

where U_{10} is the wind speed (m s^{-1}) 10 m above the ground and $n = 0.5$ for U_{10} greater than 3.7 m s^{-1} and $n = 0.67$ otherwise (Vachon et al. 2010). U_{10} was obtained as hourly averages from the nearby Environment Canada stations.

Although the Cole and Caraco (1998) wind model produces relatively conservative estimates of k_{600}, it likely overestimates fluxes from very small water bodies such as the melt ponds in this study. Laurion et al. (2010) found that chamber fluxes from small thermokarst

ponds were on average 2.5 times less than those estimated using the Cole and Caraco (1998) wind model. As lake size decreases, Vachon and Prairie (2013) showed a decrease in gas transfer velocity for a given wind speed, and Read et al. (2012) highlighted the increasing importance of convection over wind shear. Although the Vachon and Prairie (2013) model was not developed using very small ponds and the authors suggested that it may also overestimate fluxes for those water bodies, we also calculated fluxes using their model with a "lake" area (LA) of 3×10^{-6} km^2:

$$k_{600} = 2.51 + 1.48U_{10} + 0.39U_{10} \log_{10} \mathrm{LA}$$

Due to logistical constraints, we did not employ floating chambers to measure fluxes in these melt ponds. In addition, the floating chamber method can greatly overestimate fluxes due to disturbance of the air–water interface (Vachon et al. 2010).

Statistical analysis

To determine if there were differences in CO_2 and CH_4 flux among degradation classes, we used SAS 9.3 to construct mixed effects models. Specifically, we used the GLIMMIX procedure and modelled site (Arctic and subarctic) and treatment (degradation class) and their interaction as fixed effects and individual plots as a random effect. Since the distribution of CH_4 flux values and model residuals indicated that CH_4 flux was not normally distributed, a lognormal distribution was used in these models. To test for differences among degradation classes and sites when there were interactions between fixed effects, we used the LSMEANS procedure to perform Tukey–Kramer adjusted multiple comparisons (Littell 2006).

Results

Melt ponds were supersaturated with CO_2 and CH_4 at both sites. Dissolved CO_2 concentrations ranged from 28 to 1477 μmol L^{-1} (median 367 μmol L^{-1}) and did not differ significantly between sites ($F_{1,19} = 0.27$, $p = 0.61$). Dissolved CH_4 concentrations were higher at the Arctic site where they ranged from 0.7 to 650 μmol L^{-1} (median 9.3 μmol L^{-1}) compared to 0.02–130 μmol L^{-1} (median 0.8 μmol L^{-1}) at the subarctic site, but the difference was not significant ($F_{1,19} = 1.87$, $p = 0.18$). At the Arctic site, average wind speeds were two times greater than at the subarctic site (6.1 versus 2.7 m s^{-1}) and as a result, k values varied by site and model. The linear Vachon and Prairie (2013) model resulted in lower k values (3.6 and 2.4 cm h^{-1} at the Arctic and subarctic sites, respectively) compared to the accelerating curvilinear Cole and Caraco (1998) model (5.3 and 2.4 cm h^{-1} at the Arctic and subarctic sites, respectively). As a result, there was little difference in melt pond fluxes computed with either model at the subarctic site, while Arctic site CO_2 and CH_4 fluxes were lower when using the Vachon and Prairie (2013) model (0.3 versus 0.5 μmol m^{-2} s^{-1} for CH_4 and 3.9 versus 5.7 μmol m^{-2} s^{-1} for CO_2). Given the small size and sheltered nature of the melt ponds, we carried out the remaining analyses using the Vachon and Prairie (2013) derived fluxes.

CO_2 emissions from melt ponds were significantly higher than from both polygon centres and wet troughs at both the Arctic and subarctic sites (Fig. 3A; Table 1). CH_4 emissions from the melt ponds and wet troughs at both sites were significantly higher than at polygon centres, where emissions were negligible (Fig. 3B). CH_4 emissions were greater from wet troughs and melt ponds at the Arctic site compared to the subarctic site (Fig. 3B).

Thaw depth, soil moisture, water depth, and temperature measurements collected during flux measurements all varied among the degradation classes at each site and between sites (Fig. 4). Standing water was not present in polygon centres but was present in the melt ponds at both sites. Standing water in wet troughs was on average 5.8 ± 5.8 cm

Fig. 3. Boxplots of (A) CO_2 and (B) CH_4 emissions from polygon centres (no degradation), wet troughs (moderate degradation), and melt ponds (severe degradation) in high-centred polygonal terrain at a subarctic and Arctic site. Boxes with the same letter are not statistically different (GLIMMIX, SAS).

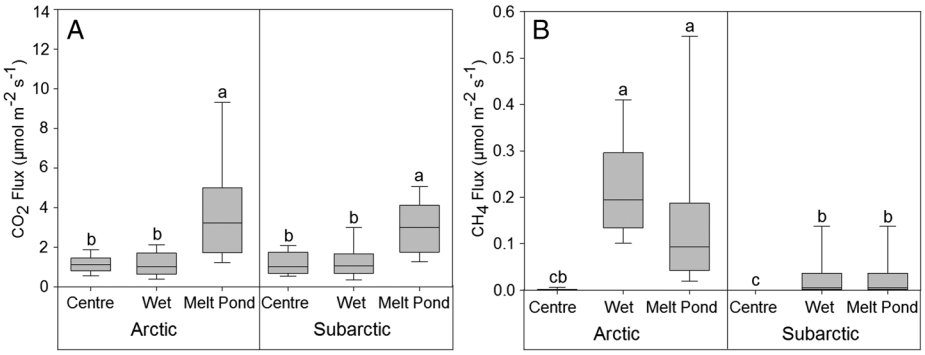

Table 1. ANOVA table from mixed effects models of CO_2 and CH_4.

	numDF	denDF	*F* value	*p* value
CO_2				
Site	1	51	0.51	0.4786
Treatment	**2**	**51**	**24.2**	**<0.0001**
Site × treatment	**2**	**51**	**0.94**	0.3958
CH_4				
Site	**1**	**64**	**40.4**	**<0.0001**
Treatment	**2**	**54**	**22.9**	**<0.0001**
Site × treatment	2	54	1.2	0.2982

Note: Fixed effects were site and treatment (degradation class). The plot sampled was included as a random effect. Significant effects are shown in bold text.

(±1 standard deviation) above the surface at the Arctic and subarctic sites. However, there was large variation in the depth of melt ponds between the Arctic and subarctic sites; standing water was 61.2 ± 23.2 cm deep at the Arctic site but only 17.3 ± 8.1 cm deep at the subarctic site (Fig. 4B). Volumetric moisture levels were typically less than 40% in polygon centres, while wet troughs were fully or nearly fully saturated (>70%) at all of the Arctic site plots and all but one plot in the subarctic site (Fig. 4D; Table 2). At both sites, thaw depth increased with increasing degradation, although differences among degradation classes were not always significant (Fig. 4C; Table 2).

In the subarctic, subsidence created deeper ponds (59.3 ± 25.5 cm) than at the Arctic site (43.0 ± 18.8 cm). Ground temperature at the base of melt ponds did not differ between the two research sites, but centres and wet troughs were cooler at the Arctic site (Fig. 4A). Ground temperatures at the base of these ponds were higher than at the polygon centres at both Arctic and subarctic sites.

Continuous temperature data from thermistors demonstrated that polygon centres had the coldest annual temperatures followed by wet troughs and then melt ponds (Table 3; Fig. 5). This difference in annual temperature was mirrored in the length of thaw season. Polygon centres were unfrozen for 23 fewer days in 2013 compared to the melt ponds, although the melt ponds thawed latest in the summer (Table 3). Wet troughs were unfrozen

Fig. 4. Soil properties in high-centred polygonal terrain in the Arctic and subarctic measured in three degradation classes (polygon centres, wet troughs, and melt ponds). (A) Ground (or water) temperature during sampling from 5 cm from the top of the soil or the top of the standing water. (B) Depth of standing water; NA indicates that no water table level was present in the active layer in polygon centres. (C) Thaw depth measured in August 2012 (not from the exact locations measured in 2013 and shown in Figs. 4A, 4B, and 4D). (D) Volumetric water content. Boxes with the same letters are not statistically different.

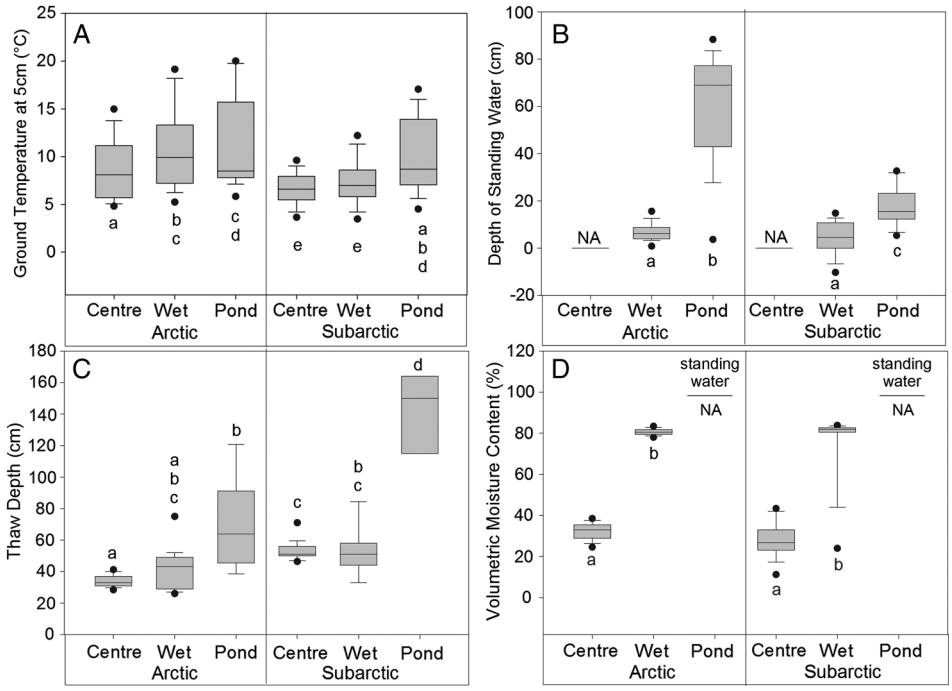

Table 2. ANOVA tables for general linear models of ground temperature during chamber measurements, water table levels, active layer thickness, and volumetric soil moisture.

	Source	DF	Type 1 SS	Mean square	*F* value	**Pr > *f***
Ground temperature	Treatment	**2**	**671.5**	**335.8**	**29.9**	**<0.0001**
	Site	**1**	**1161.5**	**1161.5**	**103.5**	**<0.0001**
	Site × treatment	**2**	**86.4**	**43.2**	**3.9**	**0.0218**
Water depth	Treatment	**1**	**38 448.6**	**38 448.6**	**242.8**	**<0.0001**
	Site	**1**	**13 475.3**	**13 475.3**	**85.1**	**<0.0001**
	Site × treatment	**1**	**13 377.9**	**13 377.9**	**84.5**	**<0.0001**
Thaw depth	Treatment	**2**	**19 659.3**	**9829.7**	**57.1**	**<0.0001**
	Site	**1**	**11 488.3**	**11 488.3**	**66.7**	**<0.0001**
	Site × treatment	**2**	**7141.1**	**3570.5**	**20.7**	**<0.0001**
Soil moisture	Treatment	**2**	**102 872.3**	**51 436.2**	**592.0**	**<0.0001**
	Site	**1**	**757.1**	**757.1**	**8.7**	**0.0037**
	Site × treatment	2	42.8	21.4	0.3	0.7821

Note: Significant effects are shown in bold.

for 12 days longer than polygon centres (Table 3). Daily average soil temperature (at 5 and 50 cm depths) was the most variable in the polygon centre at the Arctic site, which had the warmest average growing season (1 June – 31 August) temperature at 5 cm (7.8 °C) and the coldest average winter temperature (1 December – 31 March) at 5 cm (–19.4 °C) of the

Table 3. Freeze and thaw dates estimated using thermistor data (August 2012 – August 2014) collected from the Arctic field site at 5 cm depth.

Degradation class	Thaw date 2013 (5 cm)	Freeze date 2013 (5 cm)	Thaw season length (days)	Average annual temperature (°C)	Average growing season temperature (°C)	Average winter temperature (°C)
Polygon centre	24 May 2013	8 October 2013	137	−6.28	7.80	−19.37
Wet trough	28 May 2013	27 October 2013	149	−4.00	4.47	−11.79
Melt pond	1 June 2013	8 November 2013	160	−0.40	2.80	−1.34

Note: Thaw dates were defined as the day when the temperature rose above 0 °C for three consecutive days. Thaw season was calculated as the number of days between thaw and freeze dates at 5 cm. Average temperatures were calculated using 5 cm depth and the growing season and winter seasons were defined as 1 June – 31 August and 1 December – 31 March.

Fig. 5. Average daily temperature (2013) at 5 cm (left) and 50 cm (right) in the soil of a polygon centre, wet trough, and melt pond at the Arctic site near Tuktoyaktuk. The dashed reference line shows 0°.

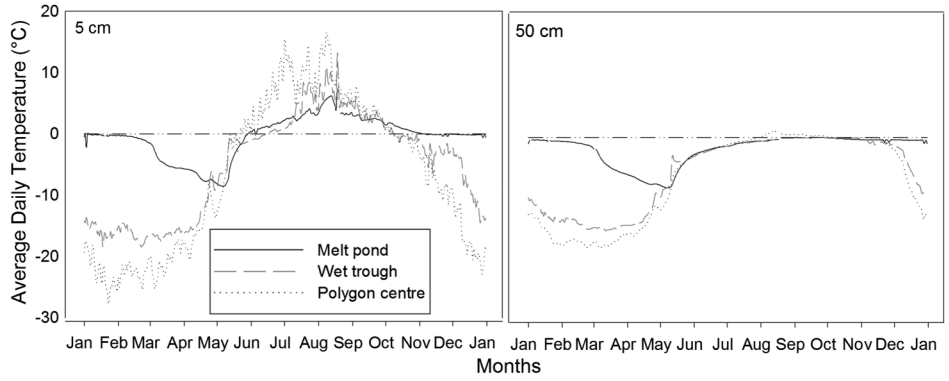

three degradation classes (Fig. 5; Table 3). Melt ponds had the least temperature variation at 5 cm below the ground surface (below 39 ± 28 cm of water) over the year with coolest soils in the growing season (2.8 °C) and the warmest winter temperatures (−1.3 °C).

Discussion

Impact of ice wedge thermokarst on carbon flux

Our data indicate that increased ice wedge degradation in high-centreed polygonal terrain will result in increased CO_2 and CH_4 emissions. However, the impact is much greater on CH_4 than on CO_2 emissions with an average of 17 times more CH_4 emitted from melt ponds and wet troughs compared to only three times more CO_2 emitted from melt ponds compared to polygon centres and wet troughs. Despite the potential of minor variation due to differences in gas sampling methods (Laurion et al. 2010), the magnitude of the trend observed far exceeds any variation attributable to sampling method and provides strong support for our overall conclusion. Even accounting for the average overestimation by a factor of 2.5 (Laurion et al. 2010), the observed increase in CH_4 and CO_2 production in melt ponds would still be 6.8 and 1.2 times that of polygon centres. A recent aerial photograph analysis suggests that the area of melt ponds in the Tuktoyaktuk Coastlands has increased by approximately 20 ha since 1972 (Steedman et al. 2017). Studies from other regions also show that the size of and number of melt ponds are increasing across the Arctic (Jorgenson et al. 2015; Lara et al. 2015;

Liljedahl et al. 2016). Taken together, these observations indicate that ice wedge thermokarst will increase total carbon emission from this terrain type. The variability that we observed among sites (Arctic versus subarctic) indicates that accurately quantifying this contribution requires additional field research to characterize variability among sites.

Greater CO_2 and CH_4 emissions from degraded ice wedge troughs relative to the polygon centres were likely caused by the combined positive effects of greater soil moisture, warmer ground temperature, and greater thaw depth and substrate availability on microbial activity. Since ice wedge degradation results in changes to moisture, temperature, and active layer thickness, our data cannot be used to isolate the mechanism responsible for increased emissions. However, previous research in Arctic peatlands suggests that increased temperature, moisture, and thaw depth may have all contributed to increased carbon mineralization at our sites (Christensen et al. 1995; Mikan et al. 2002; Oberbauer et al. 2007; Elberling et al. 2008; Zona et al. 2012). We did not measure variation in organic matter quality within our sites, but a study by Vardy et al. (1997) showing variation in percent organic matter across an area of high-centreed polygonal terrain northeast of Tuktoyaktuk raises the possibility that substrate heterogeneity could also be contributing to the differences in emission that we measured. Increased active layer thickness in melt ponds and wet troughs caused by ice wedge thaw may have also increased the available pool of organic carbon for mineralization. The results from incubations using peat from our Arctic site (Martin 2015) demonstrate that carbon currently frozen in the permafrost is vulnerable to release when active layers deepen.

Higher CH_4 emissions in wet troughs and melt ponds compared to polygon centres were expected as a result of saturated conditions that can promote net methanogenesis (Funk et al. 1994; Davidson and Janssens 2006; Schlesinger and Bernhardt 2013). Variation in CH_4 emissions between sites may be impacted by differences in trough depth and the age of thermokarst or ice wedge degradation histories at each site. As described by Laurion et al. (2010), ponds over melting ice wedges around peat polygons, also known as runnel ponds, are humic-rich water bodies characterized by peat erosion and slumping. The Arctic site had deeper and wider melt ponds, which resulted in deeper thaw at the bottom and on the sides of troughs and likely greater inputs of allochthonous carbon through erosion (Laurion and Mladenov 2013) resulting in greater amounts of carbon substrate for mineralization, but detailed soil and water data are required to test this hypothesis. The subarctic site has relict ice wedges, which are truncated well below the current depth of thaw, suggesting that melt occurred during a warm episode in the mid-Holocene (Burn 1997; Kokelj et al. 2014). Since ice wedges degraded at these sites much earlier, it is likely that much of the easily decomposable soil organic carbon has already been mineralized leaving only more recalcitrant soil organic carbon (Grosse et al. 2011; Schmidt et al. 2011; Schädel et al. 2014). Given that benthic respiration is an important source of respired carbon in thaw ponds (Breton et al. 2009), the lability of the soil organic carbon at the bottom of the melt pond is likely an important factor influencing carbon mineralization rates.

Melt ponds in high-centred polygonal terrain in the Tuktoyaktuk Coastlands were larger sources of CO_2 and CH_4 relative to other forms of thermokarst and other northern water bodies (Kling et al. 1991; Hamilton et al. 1994; Laurion et al. 2010; Negandhi et al. 2013). CO_2 and CH_4 fluxes from the melt ponds in this study ranged from 0.07 to 44.3 mmol CO_2 m^{-2} h^{-1} (mean 12.5 ± 8.7 mmol CO_2 m^{-2} h^{-1}) and from 0.0003 to 3.63 mmol CH_4 m^{-2} h^{-1} (with one outlying reading of 22.7 mmol CH_4 m^{-2} h^{-1}, mean 0.40 ± 0.74 mmol CH_4 m^{-2} h^{-1} excluding the outlier). Lower fluxes were observed from permafrost thaw ponds in the

eastern Canadian subarctic and Arctic expressed on an hourly basis (Laurion et al. 2010: range −0.85 to 4.77 mmol CO_2 m^{-2} h^{-1}, 0.0013–0.23 mmol CH_4 m^{-2} h^{-1}; Negandhi et al. 2013: range −0.34 to 3.20 mmol CO_2 m^{-2} h^{-1}, 0.0008–0.26 mmol CH_4 m^{-2} h^{-1}), coastal Alaska (Lara et al. 2015: 1.61 ± 0.76 mmol CO_2 m^{-2} h^{-1}, 0.30 ± 0.12 CH_4 m^{-2} h^{-1}), and from nonthermokarst water bodies in Alaska (Kling et al. 1991: −0.23 to 2.50 mmol CO_2 m^{-2} h^{-1}). However, our fluxes were similar to those from wetland ponds in the Hudson Bay Lowlands (Hamilton et al. 1994: means from 3.50 to 10.41 mmol CO_2 m^{-2} h^{-1}, 0.29 to 0.47 mmol CH_4 m^{-2} h^{-1}). The high-centred polygons and wet troughs in the Tuktoyaktuk Coastlands emit less CO_2 (mean 4.30 ± 2.62 mmol CO_2 m^{-2} h^{-1}) than the average observed by Christensen et al. (2000) in a high Arctic valley (16.66 ± 1.06 mmol CO_2 m^{-2} h^{-1}) but similar to the emissions from flat/high-centreed centres, rims, and troughs in Alaska (2.90 ± 2.12, 3.38 ± 2.92, and 5.00 ± 3.34, respectively) observed by Vaughn et al. (2016) and from polygon rims (3.6 mmol CO_2 m^{-2} h^{-1}) and low-cented polygons (2.16 mmol CO_2 m^{-2} h^{-1}) observed by Zona et al. (2011). They were lower than the emissions observed by Lara et al. (2015) in Barrow, Alaska, in high- and low-centred polygons, respectively (2.46 ± 0.76 mmol CO_2 m^{-2} h^{-1} and 2.37 ± 0.76 mmol CO_2 m^{-2} h^{-1}). On average, the CH_4 emissions from our polygon centres were small (mean 0.08 ± 0.85 mmol CH_4 m^{-2} h^{-1}) but larger than the average CH_4 fluxes observed from a polygon rim (0.0127 mmol CH_4 m^{-2} h^{-1}) and high-centreed polygon (0.0273 mmol CH_4 m^{-2} h^{-1}) in Siberia by Sachs et al. (2010) and smaller than from a high-centreed polygon center (0.0018 ± 0.0036 mmol CH_4 m^{-2} h^{-1}) and rim (0.0019 ± 0.0034 mmol CH_4 m^{-2} h^{-1}) in Alaska observed by Vaughn et al. (2016). Similarly, Lara et al. (2015) also observed larger CH_4 emissions from high- and low-centred polygons, respectively, in Alaska (0.04 ± 0.01 and 0.03 ± 0.01 mmol CH_4 m^{-2} h^{-1}). Average emissions from the wet troughs in this study (0.54 ± 0.85 mmol CH_4 m^{-2} h^{-1}) were higher than those observed in a studies focussed on low-centreed polygons (0.31 ± 0.18 mmol CH_4 m^{-2} h^{-1} in Vaughn et al. (2016) and 0.20–0.26 mmol CH_4 m^{-2} h^{-1} in Sachs et al. (2010)) and high-centreed polygons (0.071 ± 0.072 mmol CH_4 m^{-2} h^{-1} in Vaughn et al. (2016)).

It is clear from this study and others (Sachs et al. 2010; Lara et al. 2015; Wainwright et al. 2015; Vaughn et al. 2016) that ice wedge degradation greatly impacts tundra and its CO_2 and CH_4 emissions. In particular, the small ponds that result from ice wedge degradation in organic soils can be important sources of CO_2 and CH_4 to the atmosphere. More research efforts are needed to understand why large variations in flux magnitudes exist to better characterize the contribution of these features to regional carbon budgets.

Key findings

1. Ice wedge thermokarst in high-centred polygonal terrain results in increased CO_2 and CH_4 emissions.
2. More widespread ice wedge thermokarst in high-centred polygonal terrain will result in increased carbon emissions.

Acknowledgements

The authors would like to thank Ciara Sharpe, Steve Kokelj, Becky Segal, and Chanda Brietzke for assistance in the field and laboratory. Funding for this project was provided by the Natural Sciences and Engineering Research Council of Canada, the Canada Foundation for Innovation, the Northwest Territories Cumulative Impact Monitoring Program, ArcticNet, the Polar Shelf Continental Project, and the University of Victoria. A.F.M. and T.C.L. conceived the study, A.F.M. and T.C.L. collected the data, A.F.M., E.R.H., and T.C.L. analysed the data, and A.F.M., T.C.L., and E.R.H. wrote the manuscript.

References

Bouchard, F., Laurion, I., Prekienis, V., Fortier, D., Xu, X., and Whiticar, M.J. 2015. Modern to millennium-old greenhouse gases emitted from ponds and lakes of the Eastern Canadian Arctic (Bylot Island, Nunavut). Biogeosciences. **12**(23): 7279–7298. doi: 10.5194/bg-12-7279-2015.

Breton, J., Vallières, C., and Laurion, I. 2009. Limnological properties of permafrost thaw ponds in northeastern Canada. Can. J. Fish. Aquat. Sci. **66**(10): 1635–1648. doi: 10.1139/F09-108.

Bubier, J.L., Moore, T.R., Bellisario, L., Comer, N.T., and Crill, P.M. 1995. Ecological controls on methane emissions from a Northern Peatland Complex in the zone of discontinuous permafrost, Manitoba, Canada. Global Biogeochem. Cycles. **9**(4): 455–470. doi: 10.1029/95GB02379.

Burn, C.R. 1997. Cryostratigraphy, paleogeography, and climate change during the early Holocene warm interval, western Arctic coast, Canada. Can. J. Earth Sci. **34**(7): 912–925. doi: 10.1139/e17-076.

Burn, C.R., and Kokelj, S.V. 2009. The environment and permafrost of the Mackenzie Delta area. Permafrost Periglac. Process. **20**(2): 83–105. doi: 10.1002/ppp.655.

Christensen, T.R., Jonasson, S., Callaghan, T.V., and Havström, M. 1995. Spatial variation in high-latitude methane flux along a transect across Siberian and European tundra environments. J. Geophys. Res. Atmos. **100**(D10): 21035–21045. doi: 10.1029/95JD02145.

Christensen, T.R., Friborg, T., Sommerkorn, M., Kaplan, J., Illeris, L., Søgaard, H., Nordstrøm, C., and Jonasson, S. 2000. Trace gas exchange in a high-Arctic valley: 1. Variations in CO_2 and CH_4 flux between tundra vegetation types. Global Biogeochem. Cycles. **14**(3): 701–713. doi: 10.1029/1999GB001134.

Cole, J.J., and Caraco, N.F. 1998. Atmospheric exchange of carbon dioxide in a low-wind oligotrophic lake measured by the addition of SF_6. Limnol. Oceanogr. **43**(4): 647–656. doi: 10.4319/lo.1998.43.4.0647.

Davidson, E.A., and Janssens, I.A. 2006. Temperature sensitivity of soil carbon decomposition and feedbacks to climate change. Nature. **440**(7081): 165–173. doi: 10.1038/nature04514. PMID: 16525463.

Dinsmore, K.J. 2008. Atmosphere-soil-stream greenhouse gas fluxes from peatlands. Ph.D. thesis, University of Edinburgh, Edinburgh, UK.

Duk-Rodkin, A., and Lemmen, D.S. 2000. Glacial history of the Mackenzie region. *In* The physical environment of the Mackenzie Valley, Northwest Territories: a base line for the assessment of environmental change. *Edited by* L.D. Dyke and L.D. Brooks. Natural Resources Canada, Geological Survey of Canada, Bulletin 547. pp. 11–20.

Elberling, B., Nordstrøm, C., Grøndahl, L., Søgaard, H., Friborg, T., Christensen, T.R., Ström, L., Marchand, F., and Nijs, I. 2008. High-arctic soil CO_2 and CH_4 production controlled by temperature, water, freezing and snow. *In* High-arctic ecosystem dynamics in a changing climate. advances in ecological research. *Edited by* H. Meltofte, T.R. Christensen, B. Eberling, M. Forchhammer, and M. Rasch. Academic Press and Elsevier. pp. 441–472.

Environment Canada. 2015. Climate data — Environment Canada. http://climate.weather.gc.ca/ [accessed 30 March 2015].

Funk, D.W., Pullman, E.R., Peterson, K.M., Crill, P.M., and Billings, W.D. 1994. Influence of water table on carbon dioxide, carbon monoxide, and methane fluxes from Taiga Bog microcosms. Global Biogeochem. Cycles. **8**(3): 271–278. doi: 10.1029/94GB01229.

Grosse, G., Harden, J., Turetsky, M., McGuire, A.D., Camill, P., Tarnocai, C., Frolking, S., Schuur, E.A.G., Jorgenson, T., Marchenko, S., Romanovsky, V., Wickland, K.P., French, N., Waldrop, M., Bourgeau-Chavez, L., and Striegl, R.G. 2011. Vulnerability of high-latitude soil organic carbon in North America to disturbance. J. Geophys. Res. Biogeosci. **116**(G4): G00K06. doi: 10.1029/2010JG001507.

Hamilton, J.D., Kelly, C.A., Rudd, J.W.M., Hesslein, R.H., and Roulet, N.T. 1994. Flux to the atmosphere of CH_4 and CO_2 from wetland ponds on the Hudson Bay lowlands (HBLs). J. Geophys. Res. Atmos. **99**(D1): 1495–1510. doi: 10.1029/93JD03020.

Hugelius, G., Strauss, J., Zubrzycki, S., Harden, J.W., Schuur, E.A.G., Ping, C.-L., Schirrmeister, L., Grosse, G., Michaelson, G.J., Koven, C.D., O'Donnell, J.A., Elberling, B., Mishra, U., Camill, P., Yu, Z., Palmtag, J., and Kuhry, P. 2014. Estimated stocks of circumpolar permafrost carbon with quantified uncertainty ranges and identified data gaps. Biogeosciences. **11**(23): 6573–6593. doi: 10.5194/bg-11-6573-2014.

Huttunen, J.T., Lappalainen, K.M., Saarijärvi, E., Väsänen, T., and Martikainen, P.J. 2001. A novel sediment gas sampler and a subsurface gas collector used for measurement of the ebullition of methane and carbon dioxide from a eutrophied lake. Sci. Total Environ. **266**(1–3): 153–158. doi: 10.1016/S0048-9697(00)00749-X. PMID: 11258835.

Jorgenson, M.T., Shur, Y.L., and Pullman, E.R. 2006. Abrupt increase in permafrost degradation in Arctic Alaska. Geophys. Res. Lett. **33**(2): L02503. doi: 10.1029/2005GL024960.

Jorgenson, M.T., Kanevskiy, M., Shur, Y., Moskalenko, N., Brown, D.R.N., Wickland, K., Striegl, R., and Koch, J. 2015. Role of ground ice dynamics and ecological feedbacks in recent ice wedge degradation and stabilization. J. Geophys. Res. Earth Surf. **120**: 2280–2297. doi: 10.1002/2015JF003602.

Kling, G.W., Kipphut, G.W., and Miller, M.C. 1991. Arctic lakes and streams as gas conduits to the atmosphere: implications for tundra carbon budgets. Science. **251**(4991): 298–301. doi: 10.1126/science.251.4991.298. PMID: 17733287.

Kokelj, S.V., and Jorgenson, M.T. 2013. Advances in thermokarst research. Permafrost Periglac. Process. **24**(2): 108–119. doi: 10.1002/ppp.1779.

Kokelj, S.V., Lantz, T.C., Wolfe, S.A., Kanigan, J.C., Morse, P.D., Coutts, R., Molina-Giraldo, N., and Burn, C.R. 2014. Distribution and activity of ice wedges across the forest–tundra transition, western Arctic Canada. J. Geophys. Res. Earth Surf. **119**(9): 2032–2047. doi: 10.1002/2014JF003085.

Kokelj, S.V., Palmer, M.J., Lantz, T.C., and Burn, C.R. 2017. Ground temperatures and permafrost warming across the forest–tundra transition, Tuktoyaktuk Coastlands and Anderson Plain, NWT, Canada. Permafrost Periglac. Process. **3**: 543–551.

Lantz, T.C., and Kokelj, S.V. 2008. Increasing rates of retrogressive thaw slump activity in the Mackenzie Delta region, N.W.T., Canada. Geophys. Res. Lett. **35**: L06502. doi: 10.1029/2007GL032433.

Lantz, T.C., Gergel, S.E., and Henry, G.H.R. 2010*a*. Response of green alder (*Alnus viridis* subsp. *fruticosa*) patch dynamics and plant community composition to fire and regional temperature in north-western Canada. J. Biogeogr. **37**(8): 1597–1610. doi: 10.1111/j.1365-2699.2010.02317.x.

Lantz, T.C., Gergel, S.E., and Kokelj, S.V. 2010*b*. Spatial heterogeneity in the shrub tundra ecotone in the Mackenzie Delta region, Northwest Territories: implications for Arctic environmental change. Ecosystems. **13**(2): 194–204. doi: 10.1007/s10021-009-9310-0.

Lantz, T.C., Steedman, A.E., Kokelj, S.V., and Segal, R.A. 2017. Inventory of polygonal terrain in the Tuktoyaktuk Coastlands, Northwest Territories. Northwest Territories Geological Survey, NWT Open Report 2016-022.

Lara, M., McGuire, A.D., Euskirchen, E.S., Tweedie, C.E., Hinkel, K.M., Skurikhin, A.N., Romanovsky, V.E., Grosse, G., Bolton, W.R., and Genet, H. 2015. Polygonal tundra geomorphological change in response to warming alters future CO_2 and CH_4 flux on the Barrow Peninsula. Glob. Change Biol. **21**: 1634–1651. doi: 10.1111/gcb.12757. PMID: 25258295.

Laurion, I., and Mladenov, N. 2013. Dissolved organic matter photolysis in Canadian arctic thaw ponds. Environ. Res. Lett. **8**(3): 035026. doi: 10.1088/1748-9326/8/3/035026.

Laurion, I., Vincent, W.F., MacIntyre, S., Retamal, L., Dupont, C., Francus, P., and Pienitz, R. 2010. Variability in greenhouse gas emissions from permafrost thaw ponds. Limnol. Oceanogr. **55**(1): 115–133. doi: 10.4319/lo.2010.55.1.0115.

Lee, H., Schuur, E.A.G., and Vogel, J.G. 2010. Soil CO_2 production in upland tundra where permafrost is thawing. J. Geophys. Res. **115**(G1): G01009. doi: 10.1029/2008JG000906.

Liljedahl, A.K., Boike, J., Daanen, R.P., Fedorov, A.N., Frost, G.V., Grosse, G., Hinzman, L.D., Iijma, Y., Jorgenson, J.C., Matveyeva, N., Necsoiu, M., Raynolds, M.K., Romanovsky, V.E., Schulla, J., Tape, K.D., Walker, D.A., Wilson, C.J., Yabuki, H., and Zona, D. 2016. Pan-Arctic ice-wedge degradation in warming permafrost and its influence on tundra hydrology. Nat. Geosci. **9**: 312–318. doi: 10.1038/ngeo2674.

Littell, R.C. 2006. SAS for mixed models. SAS Institute, Inc., Cary, N.C.

Martin, A.F. 2015. Carbon fluxes from high-centred polygonal terrain in the Northwest Territories. Masters of Science, University of Victoria, Victoria, B.C.

Mikan, C.J., Schimel, J.P., and Doyle, A.P. 2002. Temperature controls of microbial respiration in arctic tundra soils above and below freezing. Soil Biol. Biochem. **34**(11): 1785–1795. doi: 10.1016/S0038-0717(02)00168-2.

Murton, J.B. 1996. Thermokarst-lake-basin sediments, Tuktoyaktuk Coastlands, western arctic Canada. Sedimentology. **43**: 737–760. doi: 10.1111/j.1365-3091.1996.tb02023.x.

Negandhi, K., Laurion, I., Whiticar, M.J., Galand, P.E., Xu, X., and Lovejoy, C. 2013. Small thaw ponds: an unaccounted source of methane in the Canadian high Arctic. PLoS ONE. **8**(11): e78204. doi: 10.1371/journal.pone.0078204. PMID: 24236014.

Oberbauer, S.F., Tweedie, C.E., Welker, J.M., Fahnestock, J.T., Henry, G.H.R., Webber, P.J., Hollister, R.D., Walker, M.D., Kuchy, A., Elmore, E., and Starr, G. 2007. Tundra CO_2 fluxes in response to experimental warming across latitudinal and moisture gradients. Ecol. Monogr. **77**(2): 221–238. doi: 10.1890/06-0649.

Oechel, W.C., Hastings, S.J., Vourlrtis, G., Jenkins, M., Riechers, G., and Grulke, N. 1993. Recent change of Arctic tundra ecosystems from a net carbon dioxide sink to a source. Nature. **361**(6412): 520–523. doi: 10.1038/361520a0.

Rampton, V.N. 1988. Quaternary geology of the Tuktoyaktuk Coastlands, Northwest Territories. Natural Resources Canada, Geological Survey of Canada, Memoir 423.

Raynolds, M.K., Walker, D.A., Ambrosius, K.J., Brown, J., Everett, K.R., Kanevskiy, M., Kofinas, G.P., Romanovsky, V.E., Shur, Y., and Webber, P.J. 2014. Cumulative geoecological effects of 62 years of infrastructure and climate change in ice-rich permafrost landscapes, Prudhoe Bay Oilfield, Alaska. Glob. Change Biol. **20**: 1211–1224. doi: 10.1111/gcb.12500. PMID: 24339207.

Read, J.S., Hamilton, D.P., Desai, A.R., Rose, K.C., MacIntyre, S., Lenters, J.D., Smyth, R.L., Hanson, P.C., Cole, J.J., Staehr, P.A., Rusak, J.A., Pierson, D.C., Brookes, J.D., Laas, A., and Wu, C.H. 2012. Lake-size dependency of wind shear and convection as controls on gas exchange. Geophys. Res. Lett. **39**: L09405. doi: 10.1029/2012GL051886.

Sachs, T., Giebels, M., Boike, J., and Kutzbach, L. 2010. Environmental controls on CH_4 emission from polygonal tundra on the microsite scale in the Lena river delta, Siberia. Glob. Change Biol. **16**: 3096–3110. doi: 10.1111/j.1365-2486.2010.02232.x.

Schädel, C., Schuur, E.A.G., Bracho, R., Elberling, B., Knoblauch, C., Lee, H., Luo, Y., Shaver, G.R., and Turetsky, M.R. 2014. Circumpolar assessment of permafrost C quality and its vulnerability over time using long-term incubation data. Glob. Change Biol. **20**(2): 641–652. doi: 10.1111/gcb.12417. PMID: 24399755.

Schlesinger, W.H., and Bernhardt, E.S. 2013. Chapter 7 — wetland ecosystems. *In* Biogeochemistry. 3rd ed. Academic Press, Boston, Mass. pp. 233–274.

Schmidt, M.W.I., Torn, M.S., Abiven, S., Dittmar, T., Guggenberger, G., Janssens, I.A., Kleber, M., Kögel-Knabner, I., Lehmann, J., Manning, D.A.C., Nannipieri, P., Rasse, D.P., Weiner, S., and Trumbore, S.E. 2011. Persistence of soil organic matter as an ecosystem property. Nature. **478**(7367): 49–56. doi: 10.1038/nature10386. PMID: 21979045.

Schuur, E.A.G., Bockheim, J., Canadell, J.G., Euskirchen, E., Field, C.B., Goryachkin, S.V., Hagemann, S., Kuhry, P., Lafleur, P.M., Lee, H., Mazhitova, G., Nelson, F.E., Rinke, A., Romanovsky, V.E., Shiklomanov, N., Tarnocai, C.,

Venevsky, S., Vogel, J.G., and Zimov, S.A. 2008. Vulnerability of permafrost carbon to climate change: implications for the global carbon cycle. BioScience. **58**(8): 701–714. doi: 10.1641/B580807.
Schuur, E.A.G., McGuire, A.D., Schädel, C., Grosse, G., Harden, J.W., Hayes, D.J., Hugelius, G., Koven, C.D., Kuhry, P., Lawrence, D.M., Natali, S.M., Olefeldt, D., Romanovsky, V.E., Schaefer, K., Turetsky, M.R., Treat, C.C., and Vonk, J.E. 2015. Climate change and the permafrost carbon feedback. Nature. **520**(7546): 171–179. doi: 10.1038/nature14338. PMID: 25855454.
Steedman, A.E., Lantz, T.C., and Kokelj, S.V. 2017. Spatio-temporal variation in high-centre polygons and ice-wedge melt ponds, Tuktoyaktuk Coastlands, Northwest Territories. Permafrost Periglac. Process. **28**(1): 66–78. doi: 10.1002/ppp.1880.
Vachon, D., and Prairie, Y.T. 2013. The ecosystem size and shape dependence of gas transfer velocity versus wind speed relationships in lakes. Can. J. Fish. Aquat. Sci. **70**: 1757–1764. doi: 10.1139/cjfas-2013-0241.
Vachon, D., Prairie, Y.T., and Cole, J.J. 2010. The relationship between near-surface turbulence and gas transfer velocity in freshwater systems and its implications for floating chamber measurements of gas exchange. Limnol. Oceanogr. **55**(4): 1723–1732. doi: 10.4319/lo.2010.55.4.1723.
Vardy, S.R., Warner, B.G., and Aravena, R. 1997. Holocene climate effects on the development of a peatland on the Tuktoyaktuk Peninsula, Northwest Territories. Quat. Res. **47**(1): 90–104. doi: 10.1006/qres.1996.1869.
Vaughn, L.J.S., Conrad, M.E., Bill, M., and Torn, M.S. 2016. Isotopic insights into methane production, oxidation, and emissions in Arctic polygon tundra. Glob. Change Biol. **22**: 3487–3502. doi: 10.1111/gcb.13281. PMID: 26990225.
Wainwright, H.M., Dafflon, B., Smith, L.J., Hahn, M.S., Curtis, J.B., Wu, Y., Ulrich, C., Peterson, J.E., Torn, M.S., and Hubbard, S.S. 2015. Identifying multiscale zonation and assessing the relative importance of polygon geomorphology on carbon fluxes in an Arctic tundra ecosystem. J. Geophys. Res. Biogeosci. **120**: 788–808. doi: 10.1002/2014JG002799.
Wanninkhof, R. 1992. Relationship between wind speed and gas exchange over the ocean. J. Geophys. Res. Oceans. **97**(C5): 7373–7382. doi: 10.1029/92JC00188.
Weiss, R.F. 1974. Carbon dioxide in water and seawater: the solubility of a non-ideal gas. Mar. Chem. **2**(3): 203–215. doi: 10.1016/0304-4203(74)90015-2.
Zoltai, S.C., and Tarnocai, C. 1975. Perennially frozen peatlands in the western Arctic and Subarctic of Canada. Can. J. Earth Sci. **12**(1): 28–43. doi: 10.1139/e75-004.
Zona, D., Lipson, D.A., Zulueta, R.C., Oberbauer, S.F., and Oechel, W.C. 2011. Microtopographic controls on ecosystem functioning in the Arctic Coastal Plain. J. Geophys. Res. **116**(G4): G00I08. doi: 10.1029/2009JG001241.
Zona, D., Lipson, D.A., Paw U, K.T., Oberbauer, S.F., Olivas, P., Gioli, B., and Oechel, W.C. 2012. Increased CO_2 loss from vegetated drained lake tundra ecosystems due to flooding. Global Biogeochem. Cycles. **26**(2): GB2004. doi: 10.1029/2011GB004037.